

Electric-Field-Induced Segmental Reorientation in Ferroelectric Liquid Crystalline Polymers and Elastomers

S. Shilov,[†] E. Gebhard,[‡] H. Skupin,[§] R. Zentel,[‡] and F. Kremer^{*,§}

Institute of Macromolecular Compounds, Bolshoi pr., 31, 199004 St. Petersburg, Russia; BUGH Wuppertal, Institute of Materials Science and Chemistry, Gauss Str. 20, 42097 Wuppertal, Germany; and Department of Physics and Geoscience, University of Leipzig, Linnèstr. 5, 04103 Leipzig, Germany

Received June 9, 1998

ABSTRACT: Macroscopically oriented ferroelectric liquid crystalline elastomers were prepared by UV-induced cross-linking of the corresponding polymer. Time-resolved FT-IR spectroscopy is employed to analyze structure and mobility in these materials on the level of the different molecular moieties. The influence of cross-linking is analyzed in detail in its effect on the molecular motion and its time dependence in response to an external electric field. The angular excursion of the motion of the spacer in response to an external electric field is much smaller than that of the mesogen. This is in pronounced contrast to low molecular FLC. The angle between the mesogen and the spacer changes continuously during the reorientation in the Sm A phase, suggesting continuous changes in the spacer conformation. It is shown that the ferroelectric order is frozen by the cross-linking reaction. A new method is described to detect the phase transition Sm C*–Sm A in ferroelectric liquid crystalline elastomers. It is based on a direct determination of the biased rotation for the polar (carbonyl) groups being the molecular origin of the observed ferroelectricity.

Introduction

Common polymers cross-linked to networks are interesting due to their elasticity and stability in shape. Especially cross-linked liquid crystalline (LC) polymers have been studied for now almost two decades as they combine network properties and liquid crystalline order.^{1,2}

Networks exhibiting helical structures display rich electromechanical effects as for example the piezoelectric effect that was detected in cholesteric and chiral smectic C elastomers for the first time in 1990.^{3,4} There are different experimental ways known to prepare chiral smectic C polymer networks. They can be realized by a multistep mechanical deformation and cross-linking process⁵ or by a cross-linking and poling procedure⁶ of the smectic systems with multidomain structure. Alternative ways start with the orientation of low molar mass liquid crystalline mixtures⁷ or polymeric systems with a ferroelectric chiral smectic C phase⁸ which are cross-linked afterward. It was demonstrated recently that ferroelectric liquid crystalline elastomers show a piezoeffect stronger than that of piezoceramics.^{8,9} The interplay between liquid crystalline properties and rubberlike elasticity can be studied best in slightly cross-linked systems that still show ferroelectric switching in electric fields.

It has been shown recently that internal mechanical stress induced by the network formation in these systems appears to act like an external electric bias voltage.¹¹ The theoretical analysis carried out in ref 11 is based on a Landau model and does not include a consideration of the chemical structure and the influence of different molecular moieties on the reorientation behavior in an electric field. To understand the mech-

anism of ferroelectric switching in ferroelectric LC elastomers on a molecular level, the influence of network formation on the mobility of different segments in response to an external electric field must be investigated. Time-resolved Fourier transform infrared (FT-IR) spectroscopy is a powerful tool for these studies since the motion of reorientation for different chemical groups can be distinguished with this technique. With the improvements of data acquisition techniques, time resolution in a nanosecond range is available now for commercial FT-IR spectrometers.¹² Recently, this method has been used for investigating the orientation behavior of ferroelectric liquid crystalline polymers.^{13–15} In these papers the molecular orientation has been followed as the time-resolved changes in the intensity of certain IR bands with fixed polarization of the incident beam. For that reason the detailed interpretation of these experiments requires assumptions about the orientation distribution function for molecular segments and their tilt angles. In contrast, time-resolved absorption measurements carried out on a complete set of IR-beam polarizations (from 0 to 180°) provide direct information about the mutual arrangements of molecular segments. Recently, this method has been used to follow the orientation dynamics of ferroelectric monomers and dimers.^{16,17}

With the aim to elucidate the influence of network formation on the mobility of different molecular moieties, time-resolved FT-IR spectroscopy has been applied to study the motion of the reorientation for the molecular segments in ferroelectric liquid crystalline polymers and elastomers under the influence of an electric field. In the following we will use the abbreviation FLCP to describe the non-cross-linked ferroelectric polymer and FLCE to describe the cross-linked, insoluble ferroelectric LC elastomer derived from it.

Experimental Section

Materials and Sample Preparation. Chemical structure and phase transition temperatures of the investigated ferro-

* To whom correspondence should be addressed.

[†] Institute of Macromolecular Compounds.

[‡] Institute of Materials Science and Chemistry.

[§] University of Leipzig.

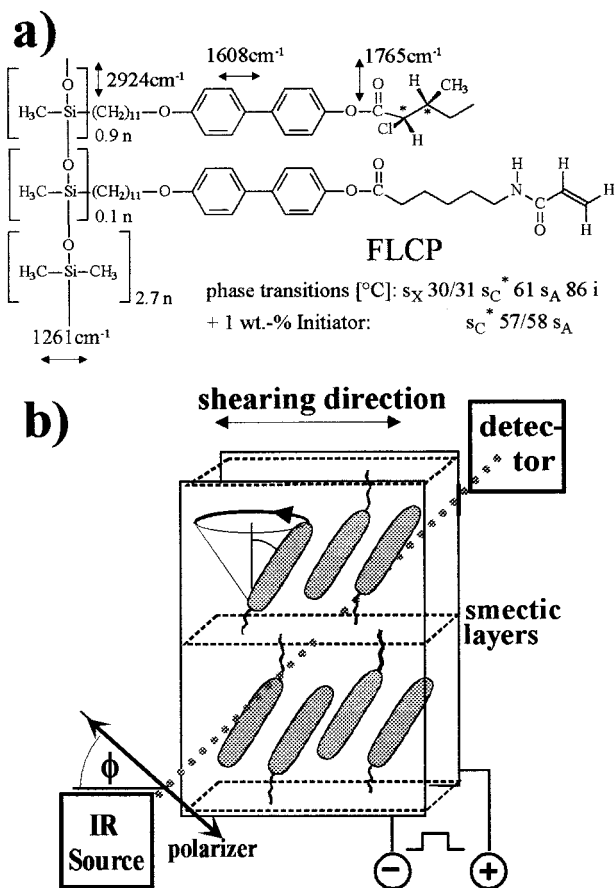


Figure 1. (a) Chemical structure and transition temperatures for the investigated FLCP/FLCE. The analyzed IR transition moments are indicated. (b) Experimental setup: the mesogens, the spacer, and the smectic layers are sketched.

electric copolysiloxane are presented in Figure 1. The phase transition temperatures were determined by polarizing microscopy, the molecular weight was determined to $M_w = 15\,200$ g/mol, and $D = 1.49$ using GPC in chloroform against polystyrene standards. The synthesis of FLCP was already published (see ref 8). The introduction of a high ratio of chiral to cross-linkable mesogenic side groups in FLCP offers the possibility to photo-cross-link the acrylamide group in the presence of an electric field using a commercial photoinitiator while retaining the ferroelectric switching process afterward. One weight percent α, α -dimethoxy- α -phenylacetophenone is added as photoinitiator to the FLCP prior to the measurements.

Our measurements were performed with a cell consisting of two parallel CaF_2 plates coated with a conductive layer of indium tin oxide. These plates are transparent from UV to the IR wavenumber range (up to 1000 cm^{-1}) and served both as windows and as electrodes. Poly(ethylene terephthalate) spacers with a thickness of $2\text{ }\mu\text{m}$ were used to maintain a well-defined spacing between the electrodes. The empty cell and the FLCP were heated to the isotropic melt, and the cell was filled by capillary forces through the gap between the windows. After filling, the cell was slowly cooled (1° C/min) at first to the Sm A phase in which the polymer was oriented by a parallel movement of one of the CaF_2 plates. An ac voltage of 20 V_{pp} (peak to peak) and 5 Hz was also applied during the shearing to reduce defects in the orientation. This procedure leads to a homogeneous orientation of the FLCP. Further cooling of the sample to the Sm C^* phase with simultaneous application of the electric field results in book-shelf orientation of the mesogens. Experiments on the orientational dynamics were carried out for both cross-linked and non-cross-linked polymers. The polymer was cross-linked by UV irradiation through the CaF_2 windows at 55° C . To keep the orientation of the molecules in one state, a dc voltage of -20 V was applied

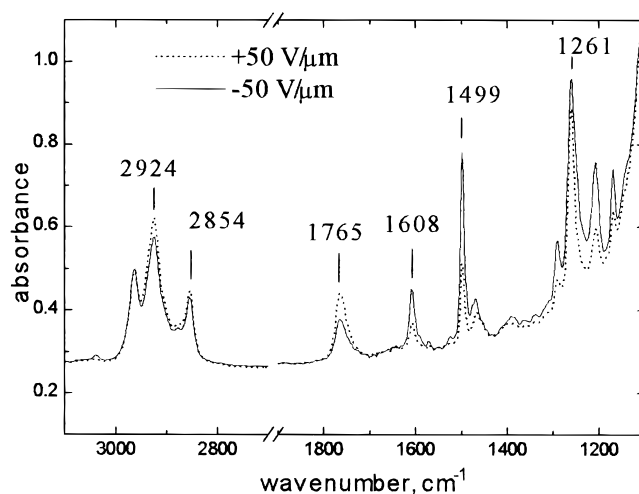


Figure 2. Infrared absorbance spectra of the FLCE for different electric field polarities. The polarization is fixed at 120° with respect to the shearing direction.

during UV irradiation. This procedure leads to the formation of the ferroelectric liquid crystalline elastomer (FLCE) with fixed orientation of the molecular segments. A high-pressure Xe lamp (150 W) with an intensity of 10 mW/cm^2 was used as UV source, and a 365 nm filter was placed in the light beam in front of the sample cell. The irradiation time was 2 min .

Measurement Technique. A FTS-6000 FT-IR (Bio-Rad, USA) spectrometer with an IR microscope (UMA-500, Bio-Rad) was used to record the IR spectra. The sample was positioned on a microscope stage using crossed polarizers for visible light, and a region of uniform orientation ($100 \times 100\text{ }\mu\text{m}^2$) was selected for the IR measurements. After the sample was positioned, the microscope was switched from the visible light mode to the IR mode. The propagation direction of the polarized IR beam was perpendicular to the plane of the windows (Figure 1). IR spectra were measured as a function of polarizer rotation angle ϕ from 0° to 170° in steps of 10° . The positions of maximal and minimal (ϕ_{max} and ϕ_{min}) absorption for different absorption bands were calculated by the center gravity method.¹⁸ With this method, the precision of determining these angles is improved to $\pm 1^\circ$. From the shift of ϕ_{max} and ϕ_{min} in response to the external electric field, the angular excursion in the position of the transition moment component perpendicular to the IR propagation is deduced. This delivers the "apparent angle" $\gamma = (\phi_{\text{max}}^{(+E)} - \phi_{\text{max}}^{(-E)})/2$.

In a static external electric field the IR spectra of the sample were recorded in the routine rapid-scan mode of the FTS-6000 with a spectral resolution of 4 cm^{-1} . To collect time-resolved spectra in course of polymer reorientation in response to an external electric field, the novel step-scan technique was used. The scheme of driving signals in step-scan mode is described elsewhere.¹⁹ Time-resolved spectra have been recorded with a time resolution of $62.5\text{ }\mu\text{s}$ and a spectral resolution of 8 cm^{-1} .

Results and Discussion

Band Assignment. Figure 2 (solid line) shows the IR spectrum of the FLCE recorded at the polarization which yield a maximal absorption of the 1608 cm^{-1} band (at an electric field strength of $-50\text{ V}/\mu\text{m}$ and a temperature of 55° C). The bands at 1608 and 1499 cm^{-1} ($\nu(\text{C}-\text{C})_{\text{ar}}$, benzene rings of the mesogen) and at 1765 cm^{-1} ($\nu(\text{C}=\text{O})$) are characteristic of the mesogenic moiety. The 2924 and 2854 cm^{-1} bands originate from asymmetric and symmetric CH_2 stretching vibrations in the polymethylene chain. Since the number of CH_2 in the tail is less than that in the spacer (which links the mesogens to the backbone), the intensity and

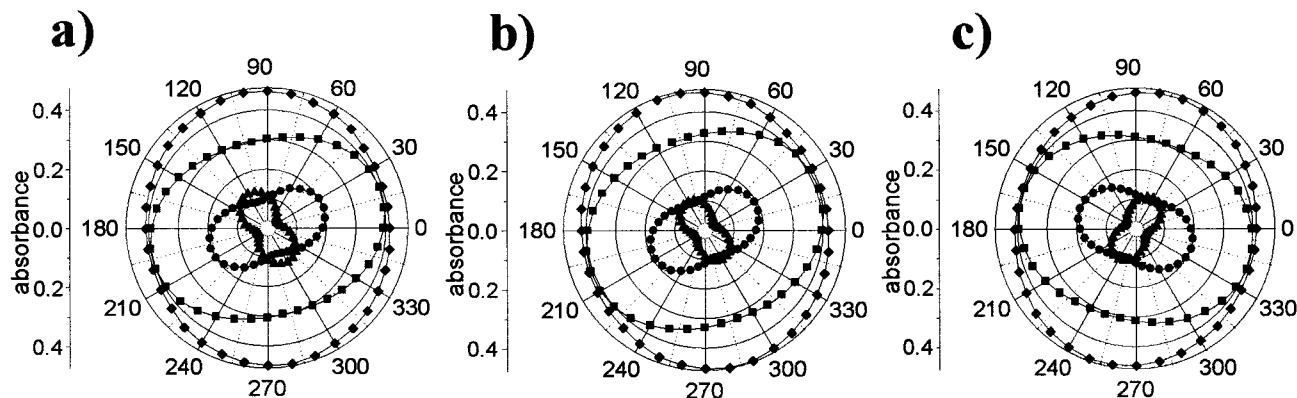


Figure 3. Polar plot of the polarizer-dependent absorbance for selected bands [\blacksquare] $\nu_{\text{as}}(\text{CH}_2)$, 2924 cm^{-1} ; [\bullet] $\nu(\text{C}=\text{O})$, 1765 cm^{-1} ; [\blacktriangle] $\nu(\text{C}-\text{C})_{\text{ar}}$, 1608 cm^{-1} ; [\blacklozenge] $\delta(\text{Si}-\text{CH}_3)$, 1261 cm^{-1}] in the FLCE under the influence of an external electric field of -50 (a), 0 (b), and $+50\text{ V}/\mu\text{m}$ (c) in the Sm C^* phase (35° C). The reversion in field polarity leads to reorientation of the different molecular groups.

dichroism of these bands mostly characterize the polymethylene spacer. To study the polysiloxane backbone, we choose the 1261 cm^{-1} band ($\delta(\text{Si}-\text{CH}_3)$). It should be mentioned that the $\nu_{\text{as}}(\text{C}-\text{O}-\text{C})$ band (related to the mesogen) also contributes to this spectral region. The spectra of the FLCP and the FLCE are similar. Unfortunately, due to the low concentration of the cross-linking component and the low intensity of the $\nu(\text{C}=\text{C})$ band, it was not possible to evaluate how many $\text{C}=\text{C}$ bonds have been converted after UV irradiation.

Orientation under the Influence of Static Electric Fields. In the Sm C^* phase of the FLCP there are two stabilized states of orientation having the mesogens inclined either to the right or to the left with respect to the smectic layer normal. The switching between these two states can be achieved by reversing the polarity of the applied electric field. The FLCP shows bistable switching in the Sm C^* phase at an electric field of $\pm 5\text{ V}/\mu\text{m}$. A higher field strength has to be applied in order to reorient the FLCE segments. Figure 2 (dotted line) shows the IR spectrum for the FLCE recorded at a field strength of $+50\text{ V}/\mu\text{m}$. The changes in the IR spectra due to the electric field polarity reflect the changes in the orientation of the molecular moieties. We found that maximal changes in the intensity are observed when the electric field rises from 0 to $40\text{ V}/\mu\text{m}$. A further increase of the electric field strength does not lead to changes in the spectra. For this reason we can conclude that an electric field strength of $50\text{ V}/\mu\text{m}$ is sufficient to reorient the molecules into the second state.

The amplitude of the molecular motion can be extracted from absorbance measurements for a complete set of polarization angles ϕ . The polar plots of the absorbance versus ϕ for selected bands are shown in parts a, b, and c of Figure 3 for -50 , 0 , and $+50\text{ V}/\mu\text{m}$, respectively. The value $\phi = 0^\circ$ in these plots is equivalent to the sample shearing direction. As can be seen from this figure, the band profiles for 0 V and negative voltage (Figure 3a,b) are nearly the same. The cross-linking has been done at negative field polarity and fixed the segmental orientation. When the polarity of the electric field is reversed, all band profiles change their position. The 1608 cm^{-1} band attains its maximum at an angle $\phi = 120^\circ$ for maximal negative voltage (Figure 3a) and at $\phi = 60^\circ$ for maximal positive voltage (Figure 3c). If it is taken into account that the transition moment for this band is nearly parallel to the mesogenic axis, the observed shift of the absorption maximum by

$\Delta\phi = 60^\circ$ corresponds to a rotation of the director by the same angle. Thus, with the $\Delta\phi/2$ value for the 1608 cm^{-1} band one already obtains the angle γ formed by the mesogens and the smectic layer normal. The value of γ_{1608} obtained from IR measurements coincides with that determined from electrooptical studies. For a further discussion of the other bands their corresponding apparent angle (or molecular excursion) values as measured in the plane perpendicular to the propagation direction of the IR beam are calculated as $\gamma = \Delta\phi/2$.

Analyzing the plots in Figure 3, one can observe that the positions of the extrema of the different bands do not coincide with each other neither for positive nor for negative voltage. With reversion of the field polarity the polar plots for the 1765 , 2924 , and 1261 cm^{-1} bands are rotated by a smaller angle than the plot for the 1608 cm^{-1} band. We obtain $\gamma_{1765} = 20^\circ$, $\gamma_{2924} = 15^\circ$, and $\gamma_{1261} = 9^\circ$ at 35° C . Similar observations have been described earlier for the case of a FLCP.¹⁵ A detailed analysis of the orientation of the molecular segments is also given in ref 15. It has been shown that the difference in the γ_{1608} and γ_{2924} values is due to the noncoincidence of the mesogenic axis and the averaged polymethylene axis. This is in contrast to nonpolymeric LC ferroelectrics where the flexible tail propagates in the direction of the mesogen axis.²⁰ The value γ_{2924} can be related to the angle formed by the averaged polymethylene axis and the smectic layer normal. The lower angle of the polymethylene axis compared to the mesogenic axis is in agreement with the zigzag model proposed for nonpolymeric smectics.^{21,22} The γ_{1261} value obtained for the polysiloxane chains indicates that the orientation of this segment also changes with the reversion of the polarity of the applied electric field, although this takes place to a smaller extent compared with the other segments. As shown in ref 23, the lower value of the apparent angle γ_{1765} for the carbonyl group results from the noncylindrical symmetry of the orientation distribution function of the $\text{C}=\text{O}$ groups around the mesogenic axis.

According to general considerations, the orientation of the mesogens in the Sm A phase is not biased, and the orientation distribution function for the mesogens has a cylindrical symmetry around the director (or smectic layer normal). In that case either the maxima or the minima (in dependence on the transition moment direction) for the different bands must coincide. Hence, in following the temperature behavior of the absorbance profiles for the 1608 and 1765 cm^{-1} bands at zero field, one can determine the transition from Sm C^* to Sm A

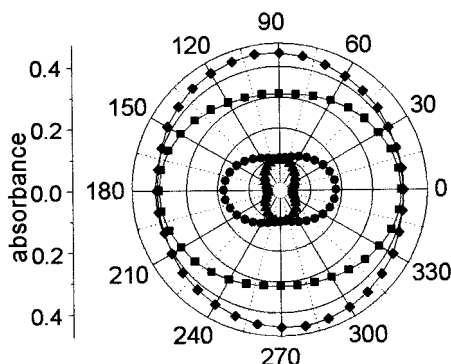


Figure 4. Polar plot for selected absorption bands [\blacksquare] $\nu_{\text{as}}(\text{CH}_2)$, 2924 cm^{-1} ; [\bullet] $\nu(\text{C}=\text{O})$, 1765 cm^{-1} ; [\blacktriangle] $\nu(\text{C}-\text{C})_{\text{ar}}$, 1608 cm^{-1} ; [\blacklozenge] $\delta(\text{Si}-\text{CH}_3)$, 1261 cm^{-1}] of FLCE in the Sm A phase, 62° C, with no field being applied. In contrast to the Sm-C* phase all polar plots have the same symmetry axes.

phase. We obtain that the distribution of the molecular segments changes from asymmetric (Figure 3b) to symmetric at 62° C (Figure 4), corresponding to the Sm C*–Sm A phase transition for investigated FLCP.

To establish the influence of cross-linking on segmental orientation, we measure the temperature dependence of the angle of excursion for the FLCP and the FLCE. The results are shown in Figure 5a,b. Comparing these two figures, one can obtain that (i) for all measured temperature intervals the absolute values of the apparent γ angles follow the relation $\gamma_{1608} > \gamma_{1765} > \gamma_{2924} > \gamma_{1261}$ for both FLCP and FLCE, (ii) the absolute values of γ are less for FLCE than that for FLCP, and (iii) the γ angles for the FLCE have nonzero values in the Sm A phase.

The difference in the γ values for the investigated bands gives evidence that the molecular segments (mesogen, spacer, and the backbone) respond to the application of the electric field to a different extent. The mesogens show the highest reorientation angle whereas the backbone has the smallest one. The difference in the absolute γ values for FLCP and FLCE can be due to the fixation of the molecular segments by the cross-linking network. The FLCP was cross-linked by UV light at a temperature close to the Sm C*–Sm A transition where the excursion angles are small (Figure 5a). The cross-linking fixed the orientation of the molecular segments closest to the network knots. As temperature decreases, the elastic forces do not allow free segmental motion in the vicinity of the network knots, which leads to lower absolute values of segmental excursions for the FLCP.

The measurement of the excursion angles for the FLCP has been done for the Sm C* phase only. The sample shows bistable switching even when a low electric field (5 V/ μm) is applied. Approaching the Sm C*–Sm A transition, the γ values for all segments drop to zero. A measurement of the induced tilt in the Sm A phase was not accomplished since it requires higher static voltages which would destroy the homogeneous alignment of the cell. In contrast to the FLCP, the alignment in the FLCE is fixed by the cross-linking which allows to measure the induced excursion angles. The results are also shown in Figure 5b. The behavior in the Sm A phase is similar to that for the Sm C* phase as the excursion angles also follow the relation $\gamma_{1608} > \gamma_{1765} > \gamma_{2924} > \gamma_{1261}$. The maximal induced γ value is observed for the mesogen and the minimal γ for the backbone. Furthermore, the relation $\gamma_{1608} > \gamma_{1765}$ shows

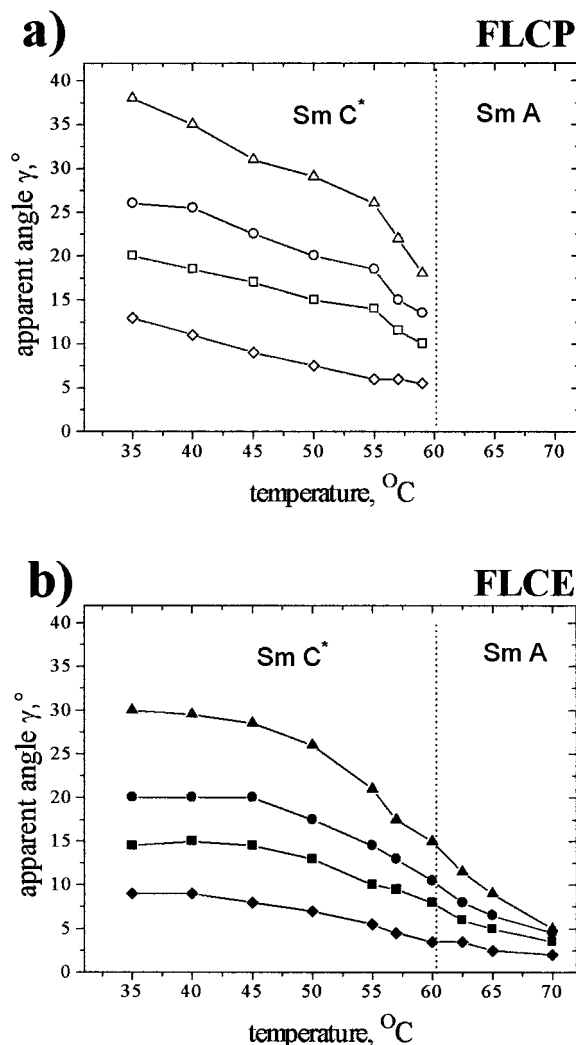


Figure 5. Temperature dependence of the apparent angles $\gamma(T)$ for the different molecular groups [\blacksquare] $\nu_{\text{as}}(\text{CH}_2)$, 2924 cm^{-1} ; [\bullet] $\nu(\text{C}=\text{O})$, 1765 cm^{-1} ; [\blacktriangle] $\nu(\text{C}-\text{C})_{\text{ar}}$, 1608 cm^{-1} ; [\blacklozenge] $\delta(\text{Si}-\text{CH}_3)$, 1261 cm^{-1}] in the FLCP (a, open symbols) and the FLCE (b, filled symbols). For the FLCP a measurement in the Sm A phase was not possible.

that the rotation of the carbonyl becomes biased in the Sm A phase when an external electric field is applied.

Orientational Dynamics in the Sm C* Phase. To compare the dynamics of the molecular reorientation in response to an electric field, we collect time-resolved FT-IR spectra at a complete set of polarization angles ϕ . Figures 6 and 7 show the time evolution of the apparent angle profiles for FLCP and FLCE when the polarity of the electric field (50 V/ μm) is reversed in the Sm C* phase at 55° C. As can be seen from these figures, the reorientation starts immediately with the reversion of the electric field polarity. The sequence $\gamma_{1608} > \gamma_{1765} > \gamma_{2924} > \gamma_{1261}$ is maintained during the reorientation (for both FLCP and FLCE) except at the point when the apparent γ values for all bands are equal to zero. We call this point the “inversion point” since all excursion angles change their sign there. The comparison of Figures 6 and 7 shows that the cross-linking has a strong influence on the response of the system. We define the reorientation time τ as the time during which the γ_{1608} angle changes from its initial value to 90% of its final value. The reorientation from the initial state in which the orientation has been fixed by the cross-linking to the second state takes more time ($\tau = 2.2$ ms)

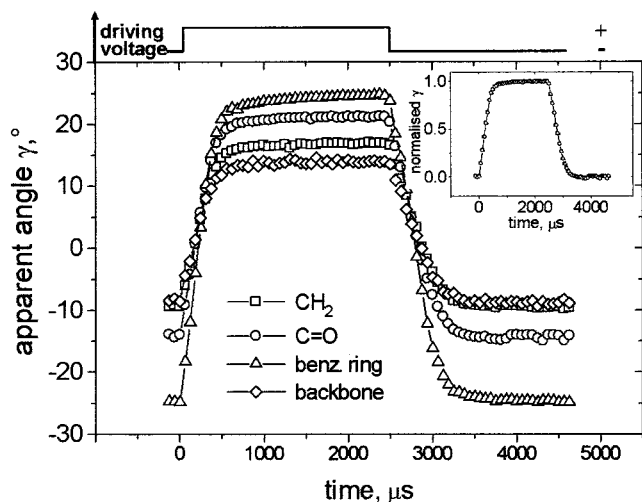


Figure 6. Time-resolved apparent angles $\gamma(t)$ for selected absorption bands of the FLCP in an electric field of ± 50 V/ μ m in Sm C* phase, 55° C. The normalization of the $\gamma(t)$ shown in the inset reveals the synchronous reorientation of the different segments.

than the relaxation back to the initial state ($\tau = 1.2$ ms). Both reorientation and relaxation time of the FLCE exceed the $\tau = 0.45$ ms value for the FLCP. A detailed analysis of the influence of the cross-linking on the switching time is given in ref 11 where it has been shown that the internal mechanical stress induced by the network formation appears to act like an external electric bias voltage. From our data we can conclude that this additional potential affects all molecular segments.

To compare the reorientation rate of different moieties, the normalized apparent angles γ_N were calculated as follows:

$$\gamma_N = (\gamma(t) - \gamma_1) / (\gamma_2 - \gamma_1) \quad (1)$$

where $\gamma(t)$ is the apparent angle at time t ; γ_1 is the value before the inversion of the polarity takes place, and γ_2 is the corresponding value after the orientation is completed. The results are plotted in the inset of Figures 6 and 7. As can be seen from these figures, the normalized curves for all bands coincide with each other with the precision of the determination of the $\gamma(t)$ values, which is $\pm 1^\circ$ for the 1604 and 2924 cm^{-1} bands and $\pm 2^\circ$ for the 1261 cm^{-1} band. This directly indicates that on the scale of microseconds the reorientation process in the Sm C* phase is a cooperative motion of all molecular segments.

Orientation Dynamics in the Sm A Phase. For the Sm A phase at 65° C the time-resolved γ profiles for selected absorption bands are shown in Figures 8 and 9 for FLCP and FLCE, respectively. The orientation time is 0.2 ms for FLCP and 0.5 ms for FLCE. The difference in orientation and relaxation is not observed in the case of the FLCE. The γ angles follow the sequence $\gamma_{1608} > \gamma_{1765} > \gamma_{2924} > \gamma_{1261}$ except at the inversion point. It should be pointed out that though the response in the Sm C* and the Sm A phase for the FLCE is similar, the mechanism of the orientation is different. It is commonly accepted that in a Sm C* phase the mesogens move on a cone in the course of the reorientation from one state to another. In this case the angle between the smectic layer normal and the mesogen is constant and does not depend on the field

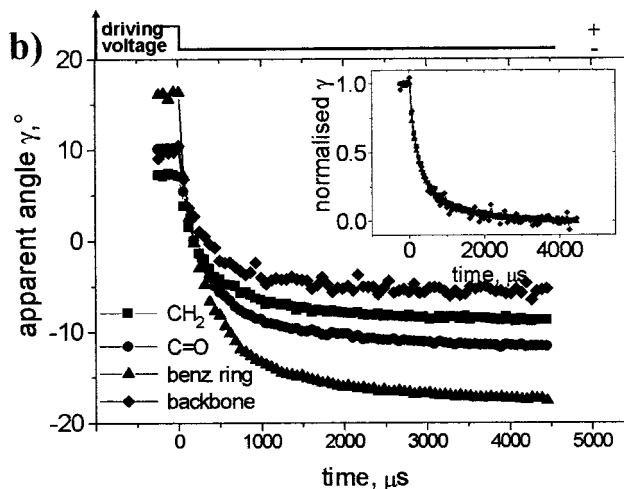
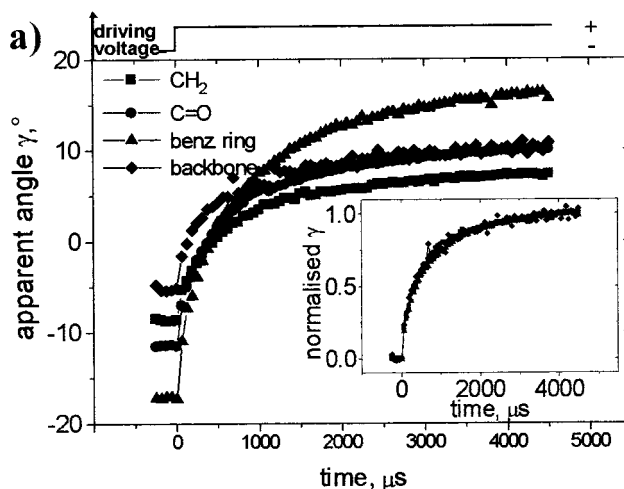


Figure 7. Orientation (a) and relaxation (b) profiles of apparent angles $\gamma(t)$ of the FLCE in response to an electric field of ± 50 V/ μ m in the Sm C* phase, 55° C. The FLCE has been cross-linked at positive polarity; the corresponding elastic energy leads to asymmetric switching behavior and to longer switching times compared to the FLCP. Inset shows normalized plots.

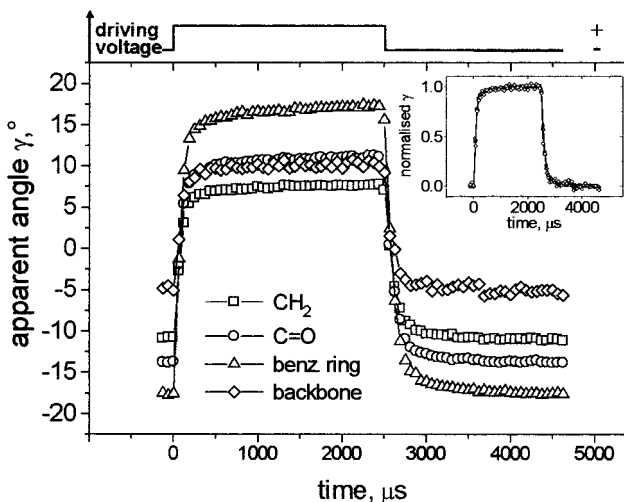


Figure 8. Time-resolved apparent angles $\gamma(t)$ for selected absorption bands of the FLCP in response to an electric field of ± 50 V/ μ m in the Sm A phase (65° C). The normalized plot is shown in the inset.

strength. In Sm A phase the mesogens move in the plane formed by the smectic layer normal and the

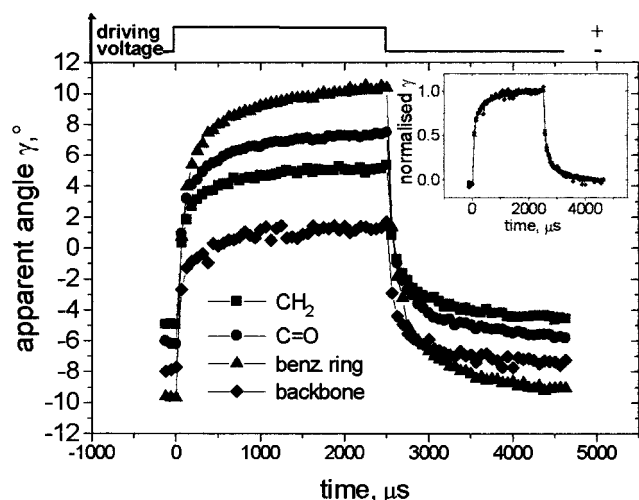


Figure 9. Time-resolved apparent angles $\gamma(t)$ for selected absorption bands of the FLCE in response to an electric field of ± 50 V/ μm in the Sm A phase (65°C). Inset shows normalized plots.

mesogen axis. In this case the tilt angle of the mesogen depends on the electric field strength. The results obtained in these studies show that in the Sm C* phase the spacer also moves on a cone but on average with a lower excursion angle than the mesogen. For the reorientation in the Sm A phase a motion is involved not only of the mesogen but also of the spacer and the backbone. At the inversion point the mesogen axis and the average spacer axis coincide with the smectic layer normal (e.g., the tilt angle of all molecular segments is zero). The external electric field induces a tilt of the mesogens which also leads to a less pronounced tilt of the spacer. The change in the difference between the excursion angles of the mesogen and the spacer (see the γ_{1608} and the γ_{2924} plots in Figures 8 and 9) in the course of the switching indicates that the molecular conformation is also varied dynamically during the reorientation. Evidently this deals with a modification of the spacer conformation, e.g., the distribution of the trans and gauche isomers along the spacer. The conformation isomerization is a fast process and cannot be followed in these experiments. It reveals a continuous changing in the angle formed by mesogen and spacer in the course of switching. Although the magnitudes of the motion for molecular segments are different, their time response is unambiguously synchronous (see insert in Figures 6–9).

Conclusions

FT-IR spectroscopic studies of FLCP and FLCE enable us to reveal the influence of cross-linking on the segmental orientation and the mobility in these systems. The highest molecular excursion in response to an external electric field is observed for the mesogens and the lowest one for the backbone in both FLCP and FLCE. Cross-linking in the Sm C* phase at temperatures close to the Sm C*–Sm A phase transition fixes the segment orientation and leads to smaller angular values for the FLCE segments as compared with FLCP.

Time-resolved FT-IR spectroscopy shows that cross-linking causes a slowing down of the motion of all molecular segments. In the course of electric-field-induced reorientation, all molecular segments move synchronously on the time scale of about 100 μs . The reorientation in the Sm A phase involves conformational changes in the polymethylene spacer as well.

A new method to find the Sm C*–Sm A transition temperature in FLCE is proposed. It is based on the measurement of the temperature dependence of polarization-dependent absorbance profiles for the carbonyl band which reflects the biased rotation of the carbonyl group around the mesogen axis.

Acknowledgment. S.V.S. acknowledges the Alexander von Humboldt foundation for fellowship and equipment donation. Support by the Innovationskolleg "Phänomene an den Miniaturisierungsgrenzen" is highly appreciated.

References and Notes

- Zentel, R. *Angew. Chem. Adv. Mater.* **1989**, *101*, 1437–1445.
- Gleim, W.; Finkelmann, H. In *Side Chain Liquid Crystal Polymers*; McArdle, C. B.; Blackie: Glasgow, 1989; pp 287–308.
- Vallerien, S. U.; Kremer, F.; Fischer, E. W.; Kapitza, H.; Zentel, R.; Poths, H.; *Macromol. Chem., Rapid Commun.* **1990**, *11*, 593–598.
- Meier, W.; Finkelmann, H. *Macromol. Chem., Rapid Commun.* **1990**, *11*, 599–605.
- Semmler, K.; Finkelmann, H. *Macromol. Chem. Phys.* **1995**, *196*, 3197–3208.
- Mauzac, M.; Nguyen, H.-T.; Tournilhac, F.-G.; Yablonsky, S.-V. *Chem. Phys. Lett.* **1995**, *240*, 461–466.
- Hikmet, R. A. M. *Macromolecules* **1992**, *25*, 5759–5764.
- Brehmer, M.; Zentel, R.; Wagenblast, G.; Siemensmeyer, K. *Macromol. Chem. Phys.* **1994**, *195*, 1891–1904.
- Eckert, T.; Finkelmann, H.; Keck, M.; Lehmann, W.; Kremer, F. *Macromol. Chem., Rapid Commun.* **1996**, *17*, 767–773.
- Lehmann, W.; Gatteringer, P.; Keck, M.; Kremer, F.; Stein, P.; Eckert, T.; Finkelmann, H. *Ferroelectrics*, in press.
- Brehmer, M.; Zentel, R.; Giesselmann, F.; Germer, R.; Zugemaier, P. *Liq. Cryst.* **1996**, *21*, 589–586.
- Johnson, T. J.; Simon, A.; Weil, J. M.; Harris, G. W. *Appl. Spectrosc.* **1993**, *47*, 1376–1381.
- Kawasaki, K.; Kidera, H.; Sekiya, T.; Hachiya, S. *Ferroelectrics* **1993**, *148*, 233–238.
- Shilov, S. V.; Okretic, S.; Siesler, H. W.; Zentel, R.; Öge, T. *Macromol. Chem., Rapid Commun.* **1995**, *16*, 125–130.
- Shilov, S. V.; Skupin, H.; Kremer, F.; Gebhard, E.; Zentel, R. *Liq. Cryst.* **1997**, *22*, 203–210.
- Hide, F.; Clark, N. A.; Nito, K.; Yasuda, A.; Walba, D. M. *Phys. Rev. Lett.* **1995**, *75*, 2344–2347.
- Shilov, S. V.; Skupin, H.; Kremer, F.; Wittig, T.; Zentel, R. *Phys. Rev. Lett.* **1997**, *79*, 1686–1689.
- Cameron, D. G.; Kauppinen, J. K.; Moffatt, D. L.; Mantsch, H. H. *Appl. Spectrosc.* **1982**, *36*, 245–252.
- Shilov, S. V.; Skupin, H.; Kremer, F.; Skarp, K.; Stein, P.; Finkelmann, H. In *Liquid Crystals: Physics, Technology and Applications*; Rutkowska, J., Ed.; *Proc. SPIE* **1998**, *3318*, 62–67.
- Kim, K. H.; Ishikawa, K.; Takezoe, H.; Fukuda, A. *Phys. Rev. E* **1995**, *51*, 2166–2175.
- Bartolino, R.; Doucet, J.; Durand, G. *Ann. Phys. (Paris)* **1978**, *3*, 389–395.
- Keller, E. N.; Nachaliel, E.; Davidov, D.; Böffel, Ch. *Phys. Rev. A* **1986**, *34*, 4363–4372.
- Miyachi, K.; Matsushima, J.; Takanishi, Y.; Ishikawa, K.; Takezoe, H.; Fukuda, A. *Phys. Rev. E* **1995**, *52*, R2153–R2156.

MA980905L